ACS Macro Letters

pubs.acs.org/macroletters Letter

Hydrolysis-Driven Viscoelastic Transition in Triblock Copolyether Hydrogels with Acetal Pendants

Jinsu Baek,[†] Seyoung Kim,*[,†] Iloh Son, Soo-Hyung Choi,* and Byeong-Su Kim*

Cite This: *ACS Macro Lett.* 2021, 10, 1080−1087 Read Online

ACCESS | Metrics & More | Article Recommendations | Supporting Information

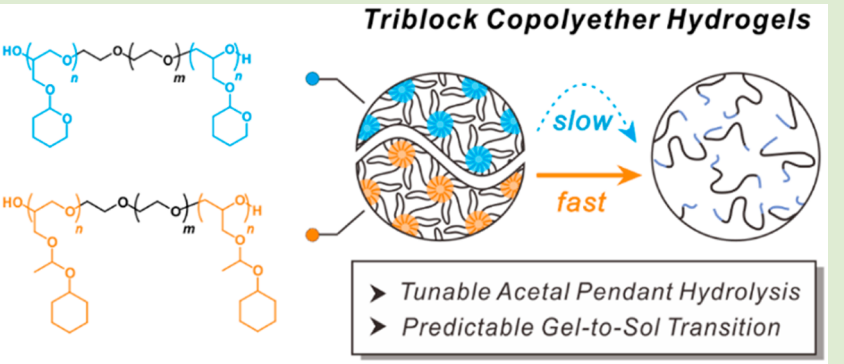

ABSTRACT: While the hydrolytic cleavage of ester groups is widely exploited in degradable hydrogels, the scission in the midst of chain backbones can bring dramatic changes in the mechanical properties of the hydrogels. However, the predictive design of the mechanical profile of the hydrogels is a complex task, mainly due to the randomness of the location of chain scission. To overcome this challenge, we herein present degradable ABA triblock poly(ethylene oxide)-based hydrogels containing an A-block bearing acetal pendant, which provides systematically tunable mechano-temporal properties of the hydrogels. In particular, hydrophobic endocyclic tetrahydropyranyl or exocyclic 1-(cyclohexyloxy)ethyl acetal pendants are gradually cleaved by acidic hydrolysis, leading to the gel-to-sol transition at room temperature. Most importantly, a series of dynamic mechanical analyses coupled with ex situ NMR spectroscopy revealed that the hydrolysis rate can be orthogonally and precisely tuned by changing the chemical structure and hydrophobicity of acetal pendants. This study provides a platform for the development of versatile degradable hydrogels in a highly controllable manner.

ABA triblock copolymers, comprising a hydrophobic A block and a hydrophilic B block, can self-assemble into hydrogels in aqueous media with mechanical and functional versatility, such as a stimuli-responsive sol−gel transition, injectability, and self-healing property.[1−3] These dynamic characteristics render the hydrogels attractive for potential biomedical and clinical use, especially for the repair of injured tissues and localized drug delivery without the need for chemical cross-linking.[4,5] In particular, hydrophobic association has been widely exploited for the preparation of dynamic hydrogels since it enables high loading capacity for hydrophobic drugs,[6,7] thermoreversible sol−gel transition near the physiological temperature,[8,9] and minimal interference with intracellular processes.[5,10] Furthermore, biodegradable hydrophobic end-blocks, such as poly(lactide-*co*-glycolide) (PLGA) and poly(ε-caprolactone) (PCL), have been extensively used for the efficient release of drugs, which is achieved by the degradation of the end-blocks upon exposure to adequate stimuli, such as pH and redox.[11,12]

Currently, the clinical use of most degradable synthetic hydrogels is based on the hydrolytic cleavage of ester groups in the polymer backbone, as in the case of PLGA and PCL.[13,14] The scission of chain backbones can cause dramatic changes in the mechanical properties of hydrogels because of the delinking of chain segments.[15,16] However, a rheological analysis of the degradable hydrogels is complicated because the hydrolytic chain scission occurs at a random location along the backbone and thus is uncontrollable. This uncertainty can be exacerbated when the end-block is copolymerized with monomers with different hydrolysis rates.[17,18] Furthermore, the lifetime of hydrophobic cores and the release profile of embedded drugs are hardly predictable, which mandates trial-and-error empirical characterizations.[19,20]

Received: June 19, 2021
Accepted: August 3, 2021

https://doi.org/10.1021/acsmacrolett.1c00413
ACS Macro Lett. 2021, 10, 1080−1087

Scheme 1. Synthesis of Tetrahydropyranyl Glycidyl Ether (TPGE) and 1-(Cyclohexyloxy)ethyl Glycidyl Ether (CHGE) Monomers, Polymerization of the Triblock Copolymers Using Poly(ethylene oxide) (PEO), and the Preparation of Hydrogels with Controllable Degradation at an Acidic pH

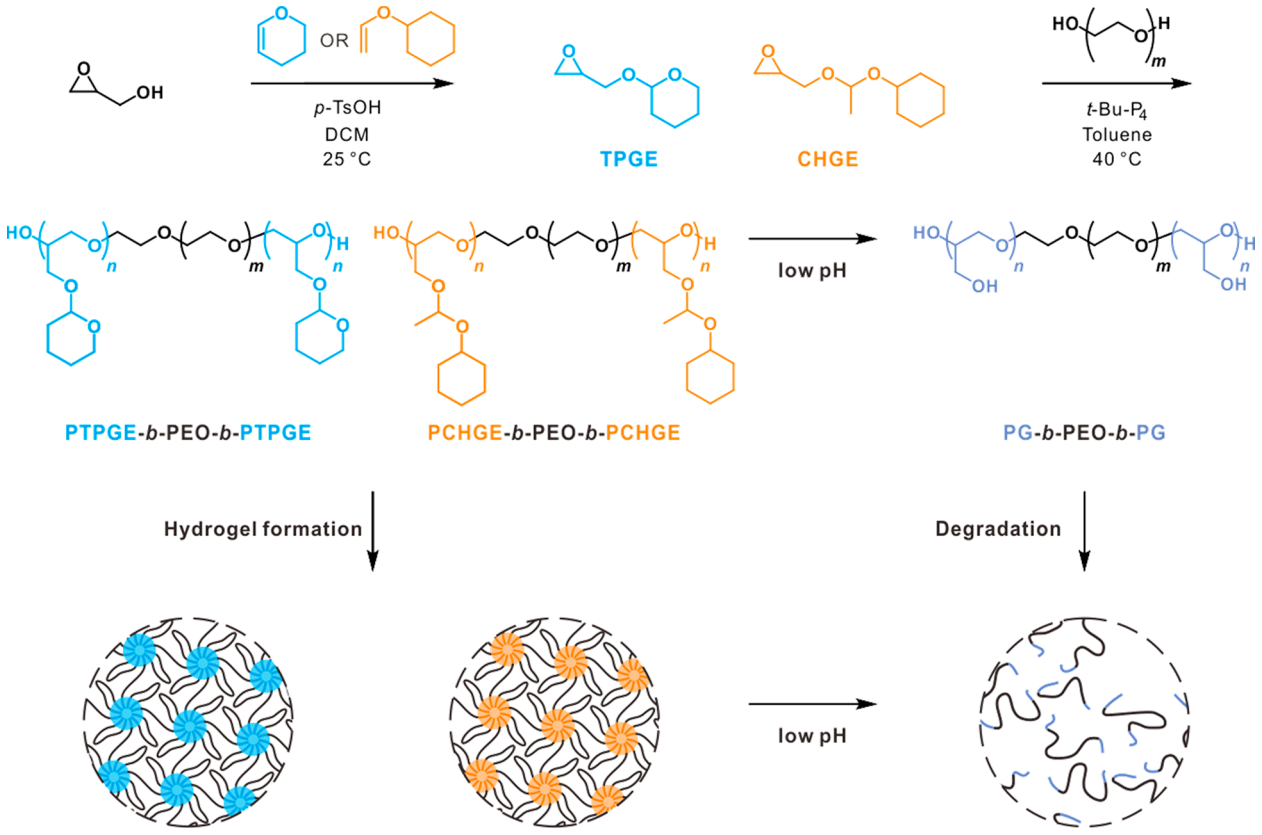

Table 1. Characterization Data for All Polymers Prepared in This Study

entry	code	polymer composition	$M_{n,end}$ [a] (g mol^{-1})	$M_{n,total}$ [b] (g mol^{-1})	$Đ$ [c]	gel [d]
1	TP_8	$PTPGE_8$-*b*-PEO_{454}-*b*-$PTPGE_8$	1300	22500	1.08	X
2	TP_{12}	$PTPGE_{12}$-*b*-PEO_{454}-*b*-$PTPGE_{12}$	1900	23800	1.09	X
3	TP_{16}	$PTPGE_{16}$-*b*-PEO_{454}-*b*-$PTPGE_{16}$	2400	24700	1.08	O
4	CH_7	$PCHGE_7$-*b*-PEO_{454}-*b*-$PCHGE_7$	1400	22800	1.07	X
5	CH_9	$PCHGE_9$-*b*-PEO_{454}-*b*-$PCHGE_9$	1800	23600	1.07	O
6	CH_{15}	$PCHGE_{15}$-*b*-PEO_{454}-*b*-$PCHGE_{15}$	3000	26000	1.08	O

[a] M_n of the end-block. [b] M_n of the overall block copolymer. [c] Dispersity ($Đ$) measured by GPC calibrated using a PEO standard in a DMF solution with 0.02 M LiCl as the eluent. [d] Gel formation was identified from the absence of flow upon inversion at 25 °C. The polymer concentrations used were 8 wt % for TP_n and 5 wt % for CH_n, respectively.

Alternatively, hydrophobic end-blocks containing cleavable pendant groups attached to the main backbone could offer controllable dynamic properties, which is ideal for both fundamental study and clinical purpose. As a representative class of cleavable pendant groups, acetal linkages can be hydrolyzed into chemically inert products under mild acidic conditions.[21,22] Several types of acetal linkages have been used as either acid-labile covalent cross-links or pendant groups.[23−25] Recently, self-assembled micelles prepared from diblock copolymers functionalized with acetal pendants have been shown to undergo highly tunable hydrolytic degradation under acidic conditions.[26−28] However, the incorporation of acetal pendants in a hydrogel-forming triblock copolymer system has not been investigated thus far.

Herein, we present polyether-based ABA triblock copolymer hydrogels containing a poly(ethylene oxide) (PEO) midblock and a hydrophobic end-block with acetal pendant groups, which provides an ideal platform to evaluate and tailor the viscoelastic transition resulting from the hydrolytic degradation of acetal pendant groups. Endocyclic acetal-based tetrahydropyranyl glycidyl ether (TPGE)[29] and exocyclic acetal-based 1-(cyclohexyloxy)ethyl glycidyl ether (CHGE)[30] were employed as two types of representative acetal pendant groups for the ABA triblock copolymers. Here, the endocyclic acetal refers to the acetal linkages that are a part of the ring structure as in TPGE.

A series of triblock copolyethers with respective acetal pendant groups were prepared via anionic ring-opening polymerization, resulting in either $PTPGE_n$-*b*-PEO-*b*-$PTPGE_n$ or $PCHGE_n$-*b*-PEO-*b*-$PCHGE_n$ (hereafter denoted by TP_n and CH_n, respectively). When dispersed in an aqueous solvent above a critical polymer concentration, the triblock copolymers formed hydrogels that underwent a dynamic gel-to-sol transition upon exposure to acidic conditions. Dynamic mechanical analysis was performed to evaluate changes in the relaxation dynamics of

https://doi.org/10.1021/acsmacrolett.1c00413
ACS Macro Lett. 2021, 10, 1080−1087

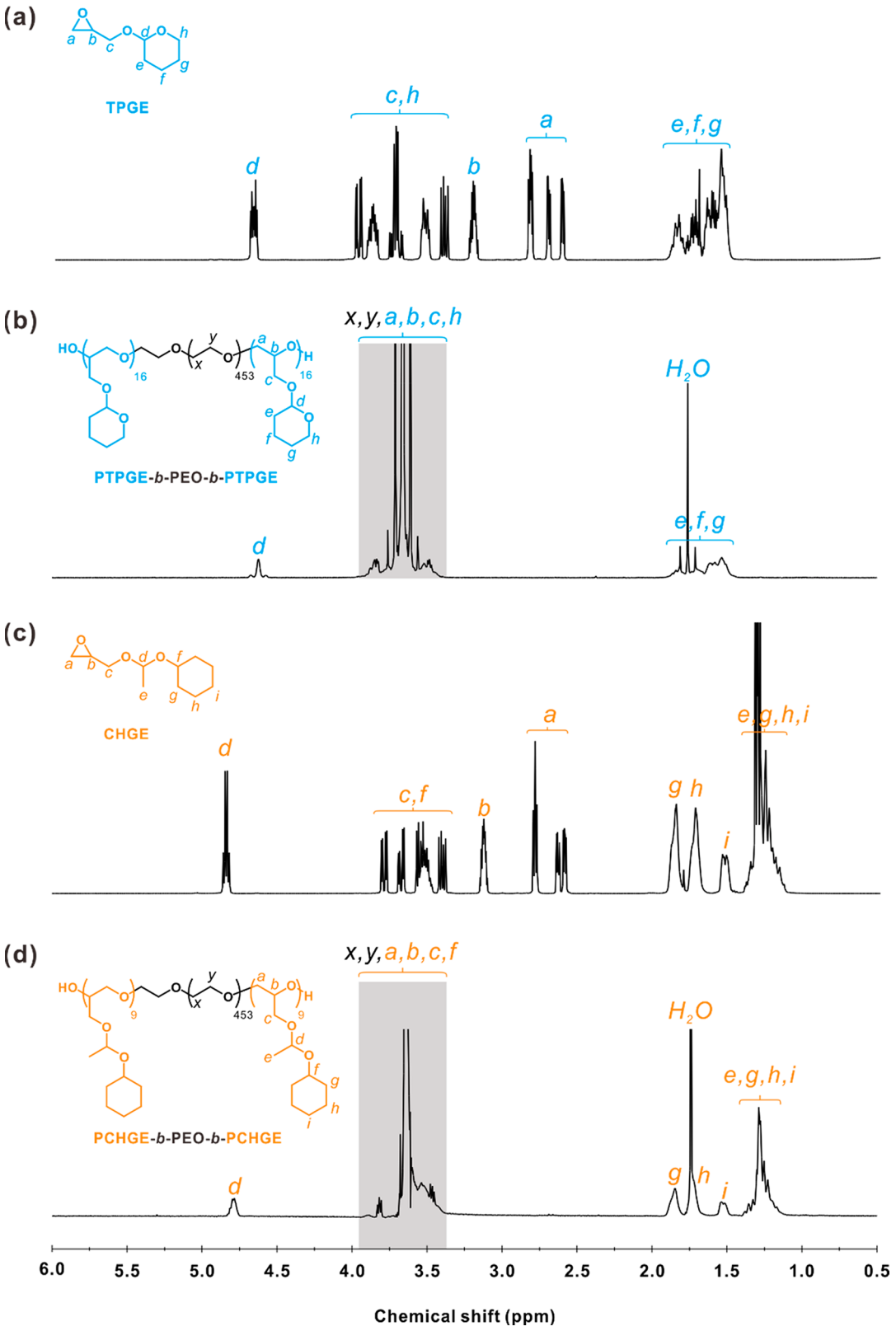

Figure 1. Representative ^{1}H NMR spectra of the (a) TPGE monomer, (b) PTPGE-*b*-PEO-*b*-PTPGE (TP_{16}, entry 3 in Table 1), (c) CHGE monomer, and (d) PCHGE-*b*-PEO-*b*-PCHGE (CH_9, entry 5 in Table 1), respectively. In panels (b) and (d), the shaded regions denote the hydrogens of the polyether backbone. All spectra were collected in $CDCl_3$ at 25 °C.

these hydrogels upon hydrolysis. Combined with ex situ NMR spectroscopy, the gel-to-sol transition is attributed to a continuous decrease in the end-block hydrophobicity by the pendant group scission, and the hydrolysis kinetics are significantly dependent on the chemical structure of the pendant groups. This study provides a new approach for the preparation of degradable block copolymer hydrogels with programmable degradation profiles.

https://doi.org/10.1021/acsmacrolett.1c00413
ACS Macro Lett. 2021, 10, 1080−1087

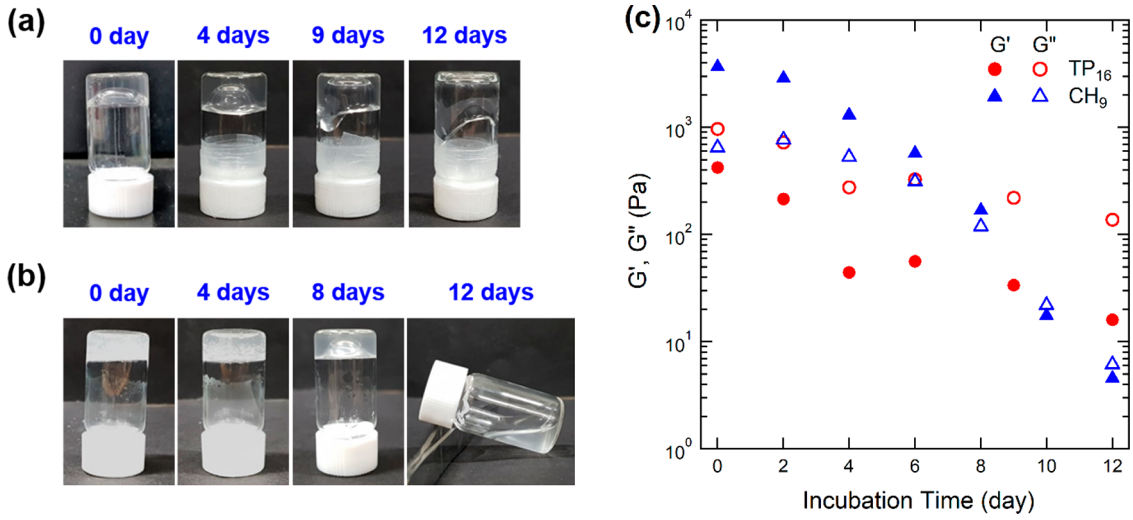

Figure 2. (a, b) Photographs of (a) TP_{16} and (b) CH_9 hydrogels at pH 5, taken after incubation at 25 °C for the target duration. Vials were inverted for 20 s before the snapshot was taken. (c) Storage modulus G' (solid) and loss modulus G'' (open), measured at a frequency of 1 Hz and a strain of 1% at 25 °C for the TP_{16} (circle) and CH_9 (triangles) hydrogels incubated at pH 5.

Hydrophobic epoxide monomers containing acetal linkages, TPGE and CHGE, were prepared by reacting glycidol with 2,3-dihydropyran and cyclohexyl vinyl ether, respectively, as previously reported by our group (Scheme 1).[29,30] Anionic ring-opening polymerization of TPGE and CHGE were performed using α,ω-hydroxy-terminated PEO (M_n = 20 kDa), resulting in a series of symmetric ABA-type triblock copolymers, as summarized in Table 1. The chemical structures of the acetal glycidyl ether monomers and the resulting triblock copolyethers were successfully resolved by ^{1}H NMR spectroscopy (Figure 1). It was found that the characteristic peaks of pendant group of the monomers are observed in the respective triblock polymers with a high polymerization conversion over 99%. The degree of polymerization (DP) and M_n of the end-block in each polymer was determined by comparing the peak area of the acetal proton (denoted as peak "*d*") to that of the polyether backbone (denoted as shaded region), as shown in Figure 1b,d. In addition, gel permeation chromatography (GPC) provided the monomodal distributions with narrow molecular weight dispersity ($Đ$ < 1.1) of all the triblock copolymers prepared. Detailed synthesis and characterization procedures can be found in the Supporting Information (Figures S1−S4).

As depicted in Scheme 1, the synthesized polymers underwent self-assembly in aqueous media to form hydrogels in which nanoscale PTPGE or PCHGE cores are interconnected by PEO midblocks. The micellar assembly of this class of ABA triblock copolymers comprising the identical PEO midblock (20 kDa) was previously documented by our group.[31] The formation of macroscopic three-dimensional networks (i.e., gelation) is generally favored for higher polymer concentrations and longer hydrophobic end-blocks.[32] This indicates the presence of a threshold DP for end-blocks above which gelation occurs at a certain polymer concentration and temperature.[31] We determined the DP of the end-blocks in both TP_n and CH_n by monitoring their gelation behavior at 8 and 5 wt % of the polymer concentrations for TP_n and CH_n, respectively. On the basis of a visual inspection after vial inversion, the threshold DPs for TP_n and CH_n were determined as 16 and 9, respectively (entries 3 and 5 in Table 1). A lower threshold DP for CH_n indicates that the PCHGE end-blocks are more hydrophobic than PTPGE end-blocks. This observation is consistent with the difference in 1-octanol/water partition coefficient (log P) estimated by the ALOGPS 2.1 program, which are 0.60 ± 0.15 and 1.82 ± 0.34 for TPGE and CHGE, respectively.[33] It is of note that the gel relaxation of CH_{15} was extremely slow due to relatively larger end-block length, and thus, we focused on the characterization of TP_{16} and CH_9 hydrogels in this study.

Figure 2 presents the viscoelastic gel-to-sol transition in TP_{16} and CH_9 hydrogels, which were prepared in 0.10 M acetate buffer at pH 5 and subjected to acidic hydrolysis at 25 °C. At different times of incubation, the images were taken 20 s after the inversion of the TP_{16} and CH_9 hydrogels to visualize viscoelastic changes (Figure 2a,b). Although both were fluidized after a long incubation time, it is evident that TP_{16} exhibited a gradual decrease in viscosity, whereas CH_9 showed an abrupt gel-to-sol transition within 8 to 12 days of incubation. This observation was corroborated by the time series measurements of dynamic moduli at 1 Hz frequency and 1% strain obtained using small-amplitude oscillatory shear measurements, as illustrated in Figure 2c. Although the storage modulus G' and loss modulus G'' decreased slowly over time for TP_{16}, those for CH_9 showed a steeper decay after a short induction period (ca. 3 days). Notably, the expected crossover between G' and G'' values at around 9 days of incubation agrees well with the time scale of the apparent gel-to-sol transition for CH_9. Consequently, CH_9 hydrogels are more solid-like than TP_{16} prior to the incubation but become more fluidic than TP_{16} as hydrolysis progresses. This reflects that the hydrolysis kinetics accompanying the transition from gel to sol upon hydrolysis is distinguished between CH_9 and TP_{16} hydrogels, which will be discussed later.

The temperature dependence of the dynamic moduli for TP_{16} hydrogel exhibited typical lower critical solution temperature (LCST) behavior (Figures S5 and S6). Both G' and G'' increased with temperature and the crossover between them occurred at 37 °C for the pristine hydrogel. Such LCST behavior has been noted in previous studies on hydrophobic interaction-driven ABA-type hydrogels, which has been attributed to the entropic effect of the hydration of hydrophobic end-blocks.[31,34] Interestingly, during hydrolysis, the crossover point shifts toward higher temperatures owing to the reduced hydrophobicity of the hydrolyzed TPGE end-block. By contrast, the

https://doi.org/10.1021/acsmacrolett.1c00413
ACS Macro Lett. 2021, 10, 1080−1087

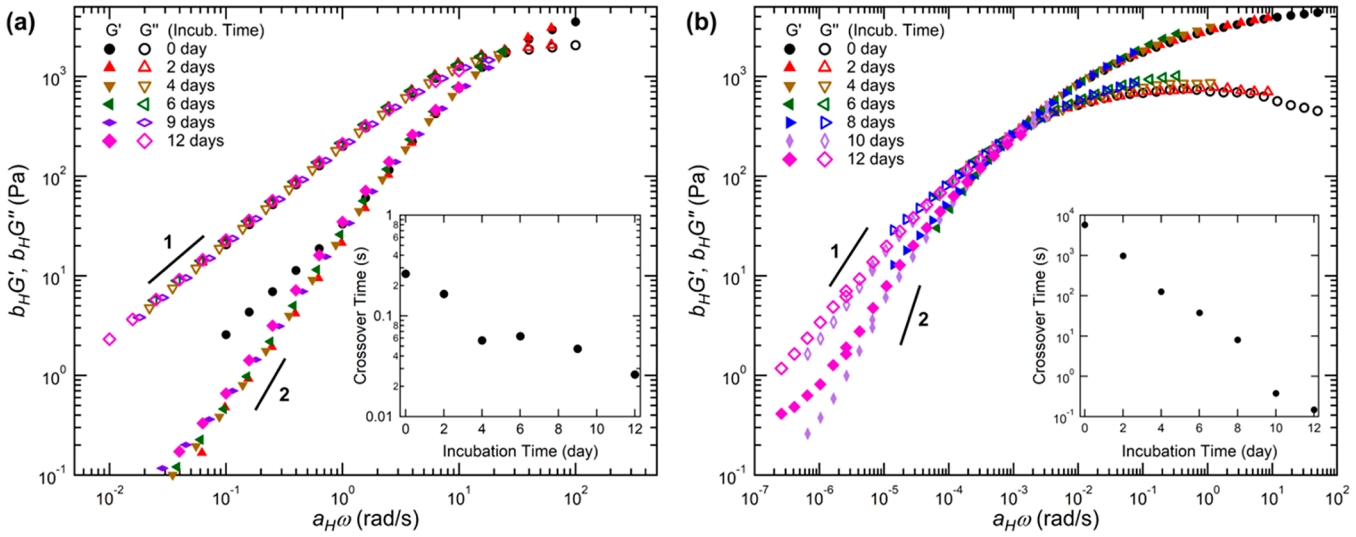

Figure 3. Time−hydrolysis superposition of the dynamic moduli G' (solid) and G'' (open). Master curves for the (a) TP_{16} and (b) CH_9 hydrogels after incubation at pH 5 and 25 °C for the target duration were obtained by using the shift factors a_H and b_H. For each curve, the initial sample without incubation (i.e., 0 day) was used as the reference. The insets show the crossover times determined from the intersection frequency of G' and G''.

CH_9 hydrogel did not exhibit LCST behavior (Figure S5b), which is possibly originated from the highly hydrophobic nature of the CHGE end-block avoiding hydration, irrespective of temperature changes. This observation is in accordance with the reported lowering of the LCST in a series of polyethers with pendant groups of high hydrophobicity.[35] While an in-depth analysis of the effect of the temperature on the structure of hydrogels is outside the scope of this study, the present results suggest that an appropriate choice of the acetal monomer allows the rational design of the LCST, which can facilitate the development of injectable hydrogels for biomedical purposes.[13]

To elucidate the mechanistic details of how the hydrolysis of the core-forming block at pH 5 affects the rheological behavior of the corresponding hydrogels, time slices of frequency-dependent dynamic moduli were measured for TP_{16} and CH_9 (Figure S7). Both spectra clearly showed a continuous decrease in G' and G'' as hydrolysis progressed. In a clear contrast, at pH 7, the prepared hydrogels did not display any noticeable changes in the dynamic moduli after prolonged incubation (~3 months), verifying that the gel-to-sol transition is significantly enhanced by the hydrolytic degradation of end-blocks in an acidic condition (Figure S8). Interestingly, we found that shifting the dynamic moduli acquired at different incubation times resulted in satisfactory superposed master curves for both TP_{16} and CH_9 in a manner analogous to the widely implemented time−temperature superposition (tTS), as shown in Figure 3.[32,36,37] The corresponding loss factors and the horizontal and vertical shift factors used to produce the master curves are displayed (Figures S9 and S10).

The apparent successful implementation of the "time−hydrolysis superposition (tHS)" practice suggests that the degree of hydrolysis regulates the hydrogel relaxation process systematically in the absence of chain backbone scission. As illustrated in Scheme 1, hydrolysis enhances the hydrophilicity of the core-forming end-blocks by cleaving the hydrophobic pendant acetal groups and leaving hydrophilic hydroxyl groups on the backbone.[29] This reduces the incompatibility between the core blocks and the aqueous medium, resulting in faster end-block expulsion from the cores and, hence, faster hydrogel relaxation.[31,38,39] Furthermore, since the DP of the end-blocks remained constant during hydrolytic cleavage in this study, the kinetics of end-block expulsion was exclusively affected by the degree of hydrolysis in every chain. This is in stark contrast to previous investigations of PLGA- or PCL-containing degradable polymer hydrogels mediated by backbone scission.[4,16] Since the position of chain scission along the backbone is inherently stochastic,[15] the quantitative control and assessment of hydrogel relaxation is difficult because of the broad molecular weight distribution of the end-blocks.

Apparently, the master curves obtained from TP_{16} and CH_9 reflect the typical behavior of viscoelastic fluids; while they show the liquid behavior (i.e., $G'' > G'$) in the low frequency limit with $G' \approx \omega^2$ and $G'' \approx \omega^1$, the solid-like behavior, such as G' plateaus (not observed within this frequency range) and $G' > G''$, is observed above a crossover frequency (ω_c).[40] The crossover time (τ) defined as $\tau = 2\pi/\omega_c$ represents the gel relaxation dynamics and the hydrolysis-time-dependent τ is clearly distinguished between TP_{16} and CH_9; CH_9 exhibited more dramatic changes in τ, which drops 5 orders of magnitude in 12 days, but τ for TP_{16} shows a drop of only 1 order of magnitude in the same period. The observed decay in τ is attributed to the enhanced hydrophilicity of the end-blocks as hydrophobic pendant groups were gradually cleaved. Upon hydrolysis, the steeper decrease in τ for CH_9 compared with the decrease for TP_{16} is partly due to the greater difference in hydrophobicity between the original and hydrolyzed pendant groups.[29] In addition, the slight overlap in τ for TP_{16} and CH_9 as the hydrolysis proceeded for 12 days strongly suggests that the hydrolysis kinetics were considerably different for TP_{16} and CH_9. This continuous and sustained decay in τ is desirable for the prediction and programming of core disintegration and for achieving control over the release profile of the hydrogels.[41]

In order to determine the hydrolysis kinetics of acetal pendant groups, ex situ ^{1}H NMR spectra of TP_{16} and CH_9 hydrogels were collected after incubation at pH 5 for a predetermined time period. The spectral regions of the acetal linkage at 4.56−4.67 and 4.75−4.80 ppm for TP_{16} and CH_9, respectively, and the polyether backbone at 3.40−3.75 ppm were displayed in Figure 4. For example, the acetal peak intensity in TP_{16} showed a slight decrease for as long as 30 days (Figure 4a). In contrast, the acetal

https://doi.org/10.1021/acsmacrolett.1c00413
ACS Macro Lett. 2021, 10, 1080−1087

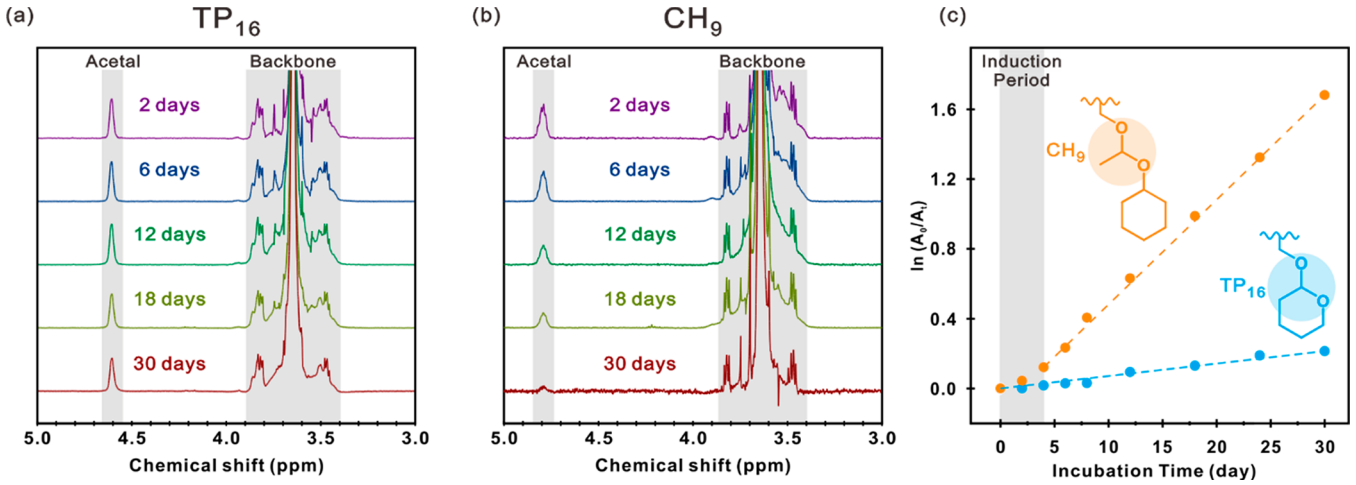

Figure 4. (a, b) Ex situ ^{1}H NMR spectra of (a) TP_{16} and (b) CH_9 over the region of acetal linkage and polyether backbone, taken after incubation at pH 5 for the target duration. (c) Reciprocal fraction of unreacted acetal pendants, A_0/A_t, determined from the ^{1}H NMR peak area for acetal groups at the beginning of incubation (A_0) and after the target incubation time (A_t). For each TP_{16} (blue) and CH_9 (yellow) hydrogel, data was fitted with first-order kinetics. The fitted lines are displayed as dashed lines with half-lives ($t_{1/2}$) of 87 and 12 days, respectively.

linkage in CH_9 is almost completely degraded during the same period, indicating considerably faster hydrolysis (Figure 4b). For a quantitative analysis, the reciprocal ratio of the number of unhydrolyzed acetal hydrogens (A_t) in the target duration to the total amount of acetal hydrogens (A_0), A_0/A_t, is plotted as a function of the hydrolysis time. Here, A_t and A_0 were obtained by comparing the integrated peak area of the acetal groups to that of the polyether backbone. The semilogarithmic representation in Figure 4c enables an analysis based on first-order kinetics, showing distinctly different hydrolysis rates with degradation half-lives ($t_{1/2}$) of 87 and 12 days for TP_{16} and CH_9, respectively.

An induction period of approximately 2−3 days was observed for CH_9, after which the hydrolysis began to follow the first-order kinetics (Figure 4c). Such induction behavior is attributed to the limited water content in the core, which comprised a hydrophobic PCHGE block in the initial stage. Previous studies suggested that hydrolytic degradation is impeded in poorly hydrated environments and that the hydrolysis of the hydrophobic segment can autoaccelerate, as the degradation product is likely to be more hydrated than the parent polymer, owing to the generated hydrophilic groups and shorter-chain molecular weight.[42−44] As the hydrolysis proceeds over 3 days, the PCHGE core becomes sufficiently hydrated, resulting in the hydration in the core not being a rate-determining factor thereafter. By contrast, no induction behavior was observed in TP_{16}, possibly due to the presence of a relatively less hydrophobic PTPGE block that allowed sufficient hydration from the onset of hydrolysis. However, the overall hydrolysis rate was higher in CH_9 compared with that of TP_{16}, despite the higher hydrophobicity of the end-block in CH_9. This can be viewed as a result of the enhanced hydrolytic stability of the endocyclic acetal linkage in TP_{16} compared with the exocyclic acetal in CH_9. The origin of the slower hydrolysis of the endocyclic acetal linkage has previously been discussed in terms of the restriction of stereoelectronically active conformations posed by the ring structure.[45] Similarly, several studies have reported a smaller entropy of cleavage for cyclic acetals because of the restriction on rotation about the breaking bond or the absence of translational entropy of the leaving group after endocyclic cleavage, which in turn resulted in a lower hydrolysis rate of cyclic acetals.[46−48] For example, cyclic dioxolane acetals were found to be hydrolyzed about 30× slower than homologous diethyl acyclic acetals.[46] Therefore, we postulate that the endocyclic acetal linkage in TPGE can significantly retard hydrolysis, thereby slowing the gel-to-sol transition kinetics of TP_{16} hydrogels to a level lower than that of CH_9.

These results imply that the triblock copolymers containing acetal pendants can serve as an ideal degradable hydrogel system with highly tunable mechano-temporal profiles. Cleaving pendant groups without backbone scission opens a new way to control the degradation profiles systematically through the copolymerization of monomers with different hydrophobicity and hydrolysis rates, in stark contrast to main-chain cleavable copolymers (e.g., PLGA and PCL), where the degradation kinetics is highly sensitive to the monomer sequence. Furthermore, the end-block length, monomer hydrophobicity, and proposed exo/endocyclic structure of acetal linkages enable the orthogonal control of the thermoresponsive behavior of hydrogels, the hydrolysis kinetics of end-blocks, and the release profile of loaded compounds in the cores. Thus, the present hydrogel systems have the superior potentials for injectable pharmaceutical hydrogels.

In summary, we present a rheological analysis of ABA-type triblock copolyether hydrogels containing cleavable acetal pendants in conjunction with a kinetic analysis of acetal hydrolysis. As the cleavage of hydrophobic pendant groups induces a continuous reduction in the hydrophobicity of the A end-blocks, the hydrogels show a decrease in the relaxation time and eventually the gel-to-sol transition occurs at room temperature. Such rheological changes are successfully described in the framework of time−hydrolysis superposition practice since the end-blocks become gradually hydrophilic as hydrolysis progresses. Furthermore, the TP_{16} hydrogels showed slower gel-to-sol transition kinetics upon hydrolysis compared with the CH_9 hydrogels, which is attributed to the constraint on endocyclic cleavage imposed by the cyclic acetal pendant groups in TP_{16}. This observation points to the orthogonal control over the elastic modulus and the softening kinetics of hydrogels by the hydrophobicity and the exo/endocyclic structure of the acetal pendant groups. Overall, our findings show that amphiphilic triblock copolymers with acetal pendant groups can facilitate the systematic tunability of the viscoelastic

https://doi.org/10.1021/acsmacrolett.1c00413
ACS Macro Lett. 2021, 10, 1080−1087

transition in hydrogels, unlike the widely used main-chain cleavable copolymer hydrogels.

■ ASSOCIATED CONTENT

Supporting Information

The Supporting Information is available free of charge at https://pubs.acs.org/doi/10.1021/acsmacrolett.1c00413.

Experimental procedure and additional characterization data. ^{13}C NMR and GPC of polymers, additional rheological analyses, and LCST behavior of hydrogels (PDF)

■ AUTHOR INFORMATION

Corresponding Authors

Byeong-Su Kim − *Department of Chemistry, Yonsei University, Seoul 03722, Republic of Korea;* orcid.org/0000-0002-6419-3054; Email: bskim19@yonsei.ac.kr

Soo-Hyung Choi − *Department of Chemical Engineering, Hongik University, Seoul 04066, Republic of Korea;* orcid.org/0000-0002-4078-6285; Email: shchoi@hongik.ac.kr

Seyoung Kim − *Department of Chemical Engineering, Hongik University, Seoul 04066, Republic of Korea;* orcid.org/0000-0002-8351-4925; Email: seyoungkim921@gmail.com

Authors

Jinsu Baek − *Department of Chemistry, Yonsei University, Seoul 03722, Republic of Korea;* orcid.org/0000-0002-6393-9176

Iloh Son − *Department of Chemistry, Yonsei University, Seoul 03722, Republic of Korea*

Complete contact information is available at: https://pubs.acs.org/10.1021/acsmacrolett.1c00413

Author Contributions

†These authors contributed equally to this work. The manuscript was written through contributions of all authors. All authors have given approval to the final version of the manuscript.

Notes

The authors declare no competing financial interest.

■ ACKNOWLEDGMENTS

This work was supported by the National Research Foundation of Korea (NRF-2021R1A2C3004978 and NRF-2021R1A2C2011164).

■ REFERENCES

(1) Zhang, M. S.; Vora, A.; Han, W.; Wojtecki, R. J.; Maune, H.; Le, A. B. A.; Thompson, L. E.; McClelland, G. M.; Ribet, F.; Engler, A. C.; Nelson, A. Dual-Responsive Hydrogels for Direct-Write 3D Printing. *Macromolecules* **2015**, *48*, 6482−6488.

(2) Tsitsilianis, C.; Serras, G.; Ko, C. H.; Jung, F.; Papadakis, C. M.; Rikkou-Kalourkoti, M.; Patrickios, C. S.; Schweins, R.; Chassenieux, C. Thermoresponsive Hydrogels Based on Telechelic Polyelectrolytes: From Dynamic to "Frozen" Networks. *Macromolecules* **2018**, *51*, 2169−2179.

(3) Tan, C. S. Y.; Liu, J.; Groombridge, A. S.; Barrow, S. J.; Dreiss, C. A.; Scherman, O. A. Controlling Spatiotemporal Mechanics of Supramolecular Hydrogel Networks with Highly Branched Cucurbit[8]uril Polyrotaxanes. *Adv. Funct. Mater.* **2018**, *28*, 1702994.

(4) Gong, C. Y.; Shi, S. A.; Wu, L.; Gou, M. L.; Yin, Q. Q.; Guo, Q. F.; Dong, P. W.; Zhang, F.; Luo, F.; Zhao, X.; Wei, Y. Q.; Qian, Z. Y. Biodegradable in Situ Gel-Forming Controlled Drug Delivery System Based on Thermosensitive PCL-PEG-PCL Hydrogel. Part 2: Sol-Gel-Sol Transition and Drug Delivery Behavior. *Acta Biomater.* **2009**, *5*, 3358−3370.

(5) Spicer, C. D. Hydrogel Scaffolds for Tissue Engineering: The Importance of Polymer Choice. *Polym. Chem.* **2020**, *11*, 184−219.

(6) Gao, Y.; Ren, F.; Ding, B.; Sun, N.; Liu, X.; Ding, X.; Gao, S. A Thermo-Sensitive PLGA-PEG-PLGA Hydrogel for Sustained Release of Docetaxel. *J. Drug Target.* **2011**, *19*, 516−527.

(7) Larrañeta, E.; Stewart, S.; Ervine, M.; Al-Kasasbeh, R.; Donnelly, R. F. Hydrogels for Hydrophobic Drug Delivery. Classification, Synthesis and Applications. *J. Funct. Biomater.* **2018**, *9*, 13.

(8) Bae, S. J.; Suh, J. M.; Sohn, Y. S.; Bae, Y. H.; Kim, S. W.; Jeong, B. Thermogelling Poly(Caprolactone-*b*-Ethylene Glycol-*b*-Caprolactone) Aqueous Solutions. *Macromolecules* **2005**, *38*, 5260−5265.

(9) Onoda, M.; Ueki, T.; Tamate, R.; Akimoto, A. M.; Hall, C. C.; Lodge, T. P.; Yoshida, R. Precisely Tunable Sol−Gel Transition Temperature by Blending Thermoresponsive ABC Triblock Terpolymers. *ACS Macro Lett.* **2018**, *7*, 950−955.

(10) Wang, F.; Bronich, T. K.; Kabanov, A. V.; Rauh, R. D.; Roovers, J. Synthesis and Evaluation of a Star Amphiphilic Block Copolymer from Poly(ε-Caprolactone) and Poly(Ethylene Glycol) as a Potential Drug Delivery Carrier. *Bioconjugate Chem.* **2005**, *16*, 397−405.

(11) Wang, P.; Chu, W.; Zhuo, X.; Zhang, Y.; Gou, J.; Ren, T.; He, H.; Yin, T.; Tang, X. Modified PLGA-PEG-PLGA Thermosensitive Hydrogels with Suitable Thermosensitivity and Properties for Use in a Drug Delivery System. *J. Mater. Chem. B* **2017**, *5*, 1551−1565.

(12) Gupta, M. K.; Martin, J. R.; Werfel, T. A.; Shen, T.; Page, J. M.; Duvall, C. L. Cell Protective, ABC Triblock Polymer-Based Thermoresponsive Hydrogels with ROS-Triggered Degradation and Drug Release. *J. Am. Chem. Soc.* **2014**, *136*, 14896−14902.

(13) Yu, L.; Ding, J. D. Injectable Hydrogels as Unique Biomedical Materials. *Chem. Soc. Rev.* **2008**, *37*, 1473−1481.

(14) Boffito, M.; Sirianni, P.; Di Rienzo, A. M.; Chiono, V. Thermosensitive Block Copolymer Hydrogels Based on Poly(ε-Caprolactone) and Polyethylene Glycol for Biomedical Applications: State of the Art and Future Perspectives. *J. Biomed. Mater. Res., Part A* **2015**, *103*, 1276−1290.

(15) Metters, A. T.; Bowman, C. N.; Anseth, K. S. A Statistical Kinetic Model for the Bulk Degradation of PLA-*b*-PEG-*b*-PLA Hydrogel Networks. *J. Phys. Chem. B* **2000**, *104*, 7043−7049.

(16) Petit, A.; Muller, B.; Bruin, P.; Meyboom, R.; Piest, M.; Kroon-Batenburg, L. M. J.; de Leede, L. G. J.; Hennink, W. E.; Vermonden, T. Modulating Rheological and Degradation Properties of Temperature-Responsive Gelling Systems Composed of Blends of PCLA-PEG-PCLA Triblock Copolymers and Their Fully Hexanoyl-Capped Derivatives. *Acta Biomater.* **2012**, *8*, 4260−4267.

(17) Li, J.; Stayshich, R. M.; Meyer, T. Y. Exploiting Sequence to Control the Hydrolysis Behavior of Biodegradable PLGA Copolymers. *J. Am. Chem. Soc.* **2011**, *133*, 6910−6913.

(18) Yu, L.; Zhang, Z.; Ding, J. D. Influence of LA and GA Sequence in the PLGA Block on the Properties of Thermogelling PLGA-PEG-PLGA Block Copolymers. *Biomacromolecules* **2011**, *12*, 1290−1297.

(19) Kitagawa, M.; Maeda, T.; Hotta, A. PEG-Based Nanocomposite Hydrogel: Thermo-Responsive Sol−Gel Transition and Degradation Behavior Controlled by the LA/GA Ratio of PLGA-PEG-PLGA. *Polym. Degrad. Stab.* **2018**, *147*, 222−228.

(20) Swider, E.; Koshkina, O.; Tel, J.; Cruz, L. J.; de Vries, I. J. M.; Srinivas, M. Customizing Poly(Lactic-*co*-Glycolic Acid) Particles for Biomedical Applications. *Acta Biomater.* **2018**, *73*, 38−51.

(21) Gillies, E. R.; Goodwin, A. P.; Fréchet, J. M. J. Acetals as pH-Sensitive Linkages for Drug Delivery. *Bioconjugate Chem.* **2004**, *15*, 1254−1263.

(22) Jazani, A. M.; Oh, J. K. Development and Disassembly of Single and Multiple Acid-Cleavable Block Copolymer Nanoassemblies for Drug Delivery. *Polym. Chem.* **2020**, *11*, 2934−2954.

(23) Murthy, N.; Thng, Y. X.; Schuck, S.; Xu, M. C.; Fréchet, J. M. J. A Novel Strategy for Encapsulation and Release of Proteins: Hydrogels and Microgels with Acid-Labile Acetal Cross-Linkers. *J. Am. Chem. Soc.* **2002**, *124*, 12398−12399.
(24) Kaihara, S.; Matsumura, S.; Fisher, J. P. Synthesis and Characterization of Cyclic Acetal Based Degradable Hydrogels. *Eur. J. Pharm. Biopharm.* **2008**, *68*, 67−73.
(25) Morinaga, H.; Morikawa, H.; Wang, Y.; Sudo, A.; Endo, T. Amphiphilic Copolymer Having Acid-Labile Acetal in the Side Chain as a Hydrophobe: Controlled Release of Aldehyde by Thermoresponsive Aggregation−Dissociation of Polymer Micelles. *Macromolecules* **2009**, *42*, 2229−2235.
(26) Zhang, Q.; Vanparijs, N.; Louage, B.; De Geest, B. G.; Hoogenboom, R. Dual pH- and Temperature-Responsive RAFT-Based Block Co-Polymer Micelles and Polymer-Protein Conjugates with Transient Solubility. *Polym. Chem.* **2014**, *5*, 1140−1144.
(27) Hwang, E.; Kim, K.; Lee, C. G.; Kwon, T. H.; Lee, S. H.; Min, S. K.; Kim, B. S. Tailorable Degradation of pH-Responsive All-Polyether Micelles: Unveiling the Role of Monomer Structure and Hydrophilic−Hydrophobic Balance. *Macromolecules* **2019**, *52*, 5884−5893.
(28) Song, J.; Hwang, E.; Lee, Y.; Palanikumar, L.; Choi, S. H.; Ryu, J. H.; Kim, B. S. Tailorable Degradation of pH-Responsive All Polyether Micelles: Via Copolymerisation with Varying Acetal Groups. *Polym. Chem.* **2019**, *10*, 582−592.
(29) Song, J.; Palanikumar, L.; Choi, Y.; Kim, I.; Heo, T. Y.; Ahn, E.; Choi, S. H.; Lee, E.; Shibasaki, Y.; Ryu, J. H.; Kim, B. S. The Power of the Ring: A pH-Responsive Hydrophobic Epoxide Monomer for Superior Micelle Stability. *Polym. Chem.* **2017**, *8*, 7119−7132.
(30) Son, I.; Lee, Y.; Baek, J.; Park, M.; Han, D.; Min, S. K.; Lee, D.; Kim, B. S. pH-Responsive Amphiphilic Polyether Micelles with Superior Stability for Smart Drug Delivery. *Biomacromolecules* **2021**, *22*, 2043−2056.
(31) Jung, H.; Gang, S. E.; Kim, J. M.; Heo, T. Y.; Lee, S.; Shin, E.; Kim, B. S.; Choi, S. H. Regulating Dynamics of Polyether-Based Triblock Copolymer Hydrogels by End-Block Hydrophobicity. *Macromolecules* **2020**, *53*, 10339−10348.
(32) Ye, Y. N.; Cui, K. P.; Indei, T.; Nakajima, T.; Hourdet, D.; Kurokawa, T.; Gong, J. P. Relaxation Dynamics and Underlying Mechanism of a Thermally Reversible Gel from Symmetric Triblock Copolymer. *Macromolecules* **2019**, *52*, 8651−8661.
(33) Tetko, I. V.; Gasteiger, J.; Todeschini, R.; Mauri, A.; Livingstone, D.; Ertl, P.; Palyulin, V. A.; Radchenko, E. V.; Zefirov, N. S.; Makarenko, A. S.; Tanchuk, V. Y.; Prokopenko, V. V. Virtual Computational Chemistry Laboratory−Design and Description. *J. Comput.-Aided Mol. Des.* **2005**, *19*, 453−463.
(34) Jeong, B.; Kim, S. W.; Bae, Y. H. Thermosensitive Sol−Gel Reversible Hydrogels. *Adv. Drug Delivery Rev.* **2012**, *64*, 154−162.
(35) Isono, T.; Miyachi, K.; Satoh, Y.; Sato, S.; Kakuchi, T.; Satoh, T. Design and Synthesis of Thermoresponsive Aliphatic Polyethers with a Tunable Phase Transition Temperature. *Polym. Chem.* **2017**, *8*, 5698−5707.
(36) Seitz, M. E.; Burghardt, W. R.; Faber, K. T.; Shull, K. R. Self-Assembly and Stress Relaxation in Acrylic Triblock Copolymer Gels. *Macromolecules* **2007**, *40*, 1218−1226.
(37) Zhang, S.; Lee, K. H.; Sun, J.; Frisbie, C. D.; Lodge, T. P. Viscoelastic Properties, Ionic Conductivity, and Materials Design Considerations for Poly(Styrene-*b*-Ethylene Oxide-*b*-Styrene)-Based Ion Gel Electrolytes. *Macromolecules* **2011**, *44*, 8981−8989.
(38) Zinn, T.; Willner, L.; Lund, R. Telechelic Polymer Hydrogels: Relation between the Microscopic Dynamics and Macroscopic Viscoelastic Response. *ACS Macro Lett.* **2016**, *5*, 1353−1356.
(39) Peters, A. J.; Lodge, T. P. Comparison of Gel Relaxation Times and End-Block Pullout Times in ABA Triblock Copolymer Networks. *Macromolecules* **2016**, *49*, 7340−7349.
(40) Annable, T.; Buscall, R.; Ettelaie, R.; Whittlestone, D. The Rheology of Solutions of Associating Polymers: Comparison of Experimental Behavior with Transient Network Theory. *J. Rheol.* **1993**, *37*, 695−726.
(41) Yoo, J.; Won, Y. Y. Phenomenology of the Initial Burst Release of Drugs from PLGA Microparticles. *ACS Biomater. Sci. Eng.* **2020**, *6*, 6053−6062.
(42) Pitt, C. G.; Shah, S. S. Manipulation of the Rate of Hydrolysis of Polymer-Drug Conjugates: The Secondary Structure of the Polymer. *J. Controlled Release* **1996**, *39*, 221−229.
(43) Gillies, E. R.; Jonsson, T. B.; Frechet, J. M. J. Stimuli-Responsive Supramolecular Assemblies of Linear-Dendritic Copolymers. *J. Am. Chem. Soc.* **2004**, *126*, 11936−11943.
(44) Yang, S. C.; Bhide, M.; Crispe, I. N.; Pierce, R. H.; Murthy, N. Polyketal Copolymers: A New Acid-Sensitive Delivery Vehicle for Treating Acute Inflammatory Diseases. *Bioconjugate Chem.* **2008**, *19*, 1164−1169.
(45) Deslongchamps, P.; Dory, Y. L.; Li, S. The Relative Rate of Hydrolysis of a Series of Acyclic and Six-Membered Cyclic Acetals, Ketals, Orthoesters, and Orthocarbonates. *Tetrahedron* **2000**, *56*, 3533−3537.
(46) Fife, T. H.; Jao, L. K. Substituent Effects in Acetal Hydrolysis. *J. Org. Chem.* **1965**, *30*, 1492−1495.
(47) Broaders, K. E.; Cohen, J. A.; Beaudette, T. T.; Bachelder, E. M.; Fréchet, J. M. J. Acetalated Dextran Is a Chemically and Biologically Tunable Material for Particulate Immunotherapy. *Proc. Natl. Acad. Sci. U. S. A.* **2009**, *106*, 5497−5502.
(48) Chen, N.; Collier, M. A.; Gallovic, M. D.; Collins, G. C.; Sanchez, C. C.; Fernandes, E. Q.; Bachelder, E. M.; Ainslie, K. M. Degradation of Acetalated Dextran Can Be Broadly Tuned Based on Cyclic Acetal Coverage and Molecular Weight. *Int. J. Pharm.* **2016**, *512*, 147−157.

https://doi.org/10.1021/acsmacrolett.1c00413
ACS Macro Lett. 2021, 10, 1080−1087